

Current fluctuations in interacting and non-interacting active particle systems

Kabir Ramola

Tata Institute of Fundamental Research,
Hyderabad, India

In collaboration with

Stephy Jose
Rahul Dandekar
Alberto Rosso

December 7, 2023

- Active systems comprising of particles that can perform directed motion by **self propulsion** constitute a major class of non-equilibrium systems.
- These systems break **detailed balance** at the local level.

Some interesting questions:

- Can **fluctuations** be studied analytically?
- What are the effects of **initial conditions** on fluctuations?
- What is the effect of **quenching initial bias directions**?
- What happens near and beyond the **motility induced phase separation**?

- 1 Non-interacting active particle model
- 2 Effect of initial conditions
- 3 Interacting active lattice gas model
- 4 Conclusions

1 Non-interacting active particle model

2 Effect of initial conditions

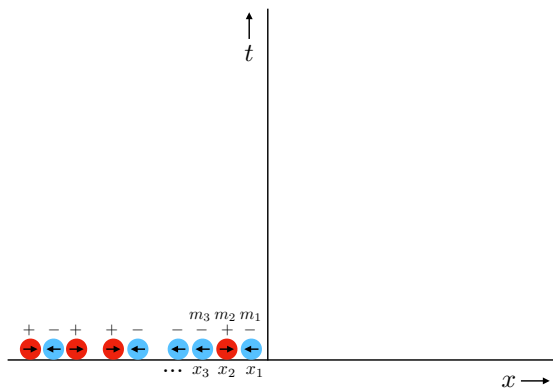
3 Interacting active lattice gas model

4 Conclusions

- We consider run and tumble particles evolving according to the **Langevin equation**

$$\frac{\partial x}{\partial t} = v\sigma(t), \quad \sigma = \pm 1. \quad (1)$$

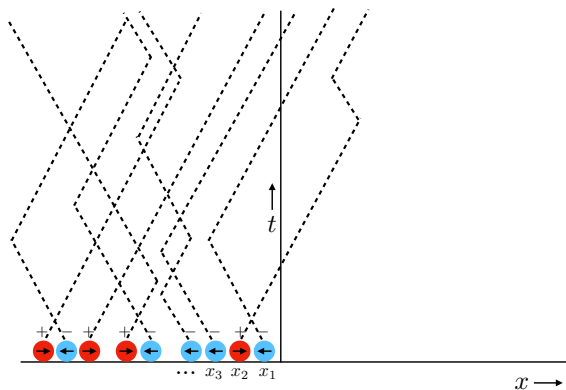
- The random variable σ switches value at a **flipping rate** γ .



Total Density = ρ

Fraction of particles in $+$ state = f_+

Fraction of particles in $-$ state = f_-



- We are interested in the flux Q of particles across the origin up to time t . We measure the **number of particles that cross the origin up to time t** = number of particles on the half infinite line ($x > 0$) at time t .
- We focus on the role of **initial conditions** on the current fluctuations.
- We start from a **step initial density** profile.
- We assume that the position of each particle is **distributed uniformly** in the box $[-L, 0]$.
- We then take a $L \rightarrow \infty$, $N \rightarrow \infty$ limit with $N/L \rightarrow \rho$ fixed in our analytical calculations.
- We consider a **fraction of particles** f_+ initialized in the $+$ state and f_- initialized in the $-$ state.

1 Non-interacting active particle model

2 Effect of initial conditions

3 Interacting active lattice gas model

4 Conclusions

Different kinds of averaging

- (1) annealed setting - average over initial realizations with mean density ρ .
- (2) quenched setting - positions of particles are fixed initially.

- The $\langle \cdots \rangle_{\{x_i\}}$ denotes an average over the history with fixed initial positions $\{x_i\}$.
- The $\overline{\cdots}$ denotes an average over initial positions.
- In the **annealed** setting, the generating function for the integrated current Q is defined as

$$\sum_{Q=0}^{\infty} e^{-\rho Q} P_{\text{an}}(Q, t) = \overline{\langle e^{-\rho Q} \rangle_{\{x_i\}}}. \quad (2)$$

- In the **quenched** setting, the generating function for the integrated current Q is defined as

$$\sum_{Q=0}^{\infty} e^{-\rho Q} P_{\text{qu}}(Q, t) = \exp \left[\ln \overline{\langle e^{-\rho Q} \rangle_{\{x_i\}}} \right]. \quad (3)$$

Different kinds of averaging (cont.)

- In the **annealed** setting, average over initial realizations with mean density ρ .

$$\overline{\langle e^{-\rho Q} \rangle_{\{x_i\}}} = 1 - \rho \overline{\langle Q \rangle_{\{x_i\}}} + \frac{\rho^2}{2} \overline{\langle Q^2 \rangle_{\{x_i\}}} + \dots \quad (4)$$

- The **cumulant generating function** is therefore

$$\ln \overline{\langle e^{-\rho Q} \rangle_{\{x_i\}}} = \underbrace{\rho \overline{\langle Q \rangle_{\{x_i\}}}}_{\mu_{\text{an}}} + \frac{\rho^2}{2} \underbrace{\left(\overline{\langle Q^2 \rangle_{\{x_i\}}} - \overline{\langle Q \rangle_{\{x_i\}}}^2 \right)}_{\sigma_{\text{an}}^2} + \dots \quad (5)$$

- In the **quenched** setting, the average is performed for every cumulant

$$\overline{\ln \langle e^{-\rho Q} \rangle_{\{x_i\}}} = \underbrace{\rho \overline{\langle Q \rangle_{\{x_i\}}}}_{\mu_{\text{qu}}} + \frac{\rho^2}{2} \underbrace{\left(\overline{\langle Q^2 \rangle_{\{x_i\}}} - \overline{\langle Q \rangle_{\{x_i\}}^2} \right)}_{\sigma_{\text{qu}}^2} + \dots \quad (6)$$

- For **non-interacting random walkers**

$$\begin{aligned}\sigma_{\text{an}}^2(t) &= \rho \sqrt{\frac{Dt}{\pi}}, \\ \sigma_{\text{qu}}^2(t) &= \rho \sqrt{\frac{Dt}{2\pi}}.\end{aligned}\tag{7}$$

- For **SSEP**

$$\begin{aligned}\sigma_{\text{an}}^2(t) &= \rho \sqrt{\frac{Dt}{\pi}} \left(1 - \frac{\rho}{\sqrt{2}}\right), \\ \sigma_{\text{qu}}^2(t) &= \rho \sqrt{\frac{Dt}{\pi}} \left(\frac{1}{\sqrt{2}} - \frac{2 - \sqrt{2}}{\sqrt{2}} \rho\right).\end{aligned}\tag{8}$$

Derrida and Gerschenfeld, Journal of Statistical Physics, 136(1):1–15, (2009).
Krapivsky and Meerson, Phys. Rev. E. 86(3):031106, (2012).

- For **non-interacting RTPs**

$$\sigma_{\text{an}}^2(t) \xrightarrow{t \rightarrow \infty} \rho \sqrt{\frac{D_{\text{eff}} t}{\pi}},$$
$$\sigma_{\text{qu}}^2(t) \xrightarrow{t \rightarrow \infty} \rho \sqrt{\frac{D_{\text{eff}} t}{2\pi}}. \quad (9)$$

$D_{\text{eff}} = v^2/(2\gamma)$ is the effective diffusion constant.

Banerjee, Majumdar, Rosso, and Schehr, Phys. Rev. E. 101(5):052101, (2020).

Di Bello, Hartmann, Majumdar, Mori, Rosso, and Schehr, Phys. Rev. E 108, 014112 (2023).

- Can the fluctuations be computed as a function of time?

RTPs: Even more, Different kinds of averaging

- The $\overbrace{\dots}$ denotes an average over initial magnetization states.
- **Annealed** density and **annealed** magnetization initial conditions

$$\sum_{Q=0}^{\infty} e^{-pQ} P_{a,a}(Q, t) = \overbrace{\langle e^{-pQ} \rangle_{\{x_i\}, \{m_i\}}} \quad (10)$$

- **Annealed** density and **quenched** magnetization initial conditions

$$\sum_{Q=0}^{\infty} e^{-pQ} P_{a,q}(Q, t) = \exp \left[\overbrace{\ln \langle e^{-pQ} \rangle_{\{x_i\}, \{m_i\}}} \right] \quad (11)$$

- **Quenched** density and **quenched** magnetization initial conditions

$$\sum_{Q=0}^{\infty} e^{-pQ} P_{q,q}(Q, t) = \exp \left[\overbrace{\ln \langle e^{-pQ} \rangle_{\{x_i\}, \{m_i\}}} \right] \quad (12)$$

- **Quenched** density and **annealed** magnetization initial conditions

$$\sum_{Q=0}^{\infty} e^{-pQ} P_{q,a}(Q, t) = \exp \left[\overbrace{\ln \langle e^{-pQ} \rangle_{\{x_i\}, \{m_i\}}} \right] \quad (13)$$

Total flux across the origin

- Let $\mathcal{I}_i(t)$ be an indicator function defined as

$$\mathcal{I}_i(t) = \begin{cases} 1, & \text{if the } i^{\text{th}} \text{ particle is to the right of the origin at time } t, \\ 0, & \text{otherwise.} \end{cases} \quad (14)$$

- The total number of particles on the right of the origin is

$$N^+ = \sum_{i=1}^N \mathcal{I}_i(t). \quad (15)$$

- For a **fixed initial realization** of the positions $\{x_i\}$ and the bias states $\{m_i\}$, the flux distribution is given as

$$P(Q, t, \{x_i\}, \{m_i\}) = \text{Prob.}(N^+ = Q) = \left\langle \delta \left[Q - \sum_{i=1}^N \mathcal{I}_i(t) \right] \right\rangle_{\{x_i\}, \{m_i\}}. \quad (16)$$

Generating Function

- We can compute the **generating function**

$$\sum_{Q=0}^{\infty} e^{-pQ} P(Q, t, \{x_i\}, \{m_i\}) = \langle e^{-pQ} \rangle_{\{x_i\}, \{m_i\}} = \left\langle \exp\left[-p \sum_{i=1}^N \mathcal{I}_i(t)\right] \right\rangle_{\{x_i\}, \{m_i\}}. \quad (17)$$

- We make use of the identity $e^{-p\mathcal{I}_i} = 1 - (1 - e^{-p})\mathcal{I}_i$ since $\mathcal{I}_i = 0, 1$.
- Since the particles are **non-interacting**, we have

$$\langle e^{-pQ} \rangle_{\{x_i\}, \{m_i\}} = \prod_{i=1}^N [1 - (1 - e^{-p}) \langle \mathcal{I}_i(t) \rangle_{\{x_i\}, \{m_i\}}]. \quad (18)$$

- This is simply expressed in terms of the single particle Green's function

$$\langle \mathcal{I}_i(t) \rangle_{\{x_i\}, \{m_i\}} = \int_0^{\infty} dx G^{m_i}(x, x_i, t) = U^{m_i}(-x_i, t), \quad x_i < 0. \quad (19)$$

- The fundamental quantity of interest is therefore

$$\langle e^{-pQ} \rangle_{\{x_i\}, \{m_i\}} = \prod_{i=1}^N [1 - (1 - e^{-p}) U^{m_i}(-x_i, t)], \quad x_i < 0. \quad (20)$$

- The evolution equations are

$$\begin{aligned}\frac{\partial P_+(x, t)}{\partial t} &= -v \frac{\partial P_+(x, t)}{\partial x} - \gamma P_+(x, t) + \gamma P_-(x, t), \\ \frac{\partial P_-(x, t)}{\partial t} &= +v \frac{\partial P_-(x, t)}{\partial x} - \gamma P_-(x, t) + \gamma P_+(x, t).\end{aligned}\tag{21}$$

- The **Green's functions** for RTP are

$$\begin{aligned}\tilde{G}(x, -z, s) &= \frac{e^{-\frac{|x+z|\sqrt{s(s+2\gamma)}}{v}} \sqrt{s(s+2\gamma)}}{2vs}, \quad z \geq 0, \\ \tilde{G}^\pm(x, -z, s) &= \frac{e^{-\frac{|x+z|\sqrt{s(s+2\gamma)}}{v}} \left(\sqrt{s(s+2\gamma)} \pm s \operatorname{sgn}(x+z) \right)}{2vs}.\end{aligned}\tag{22}$$

Single particle propagators (cont.)

- Green's function in real space are **complicated**

$$G(x, -z, t) = \frac{e^{-\gamma t}}{2} \left\{ \delta(x + z - vt) + \delta(x + z + vt) \right. \\ \left. + \frac{\gamma}{v} \left[I_0(\omega) + \frac{\gamma t I_1(\omega)}{\omega} \right] \Theta(vt - |x + z|) \right\}, \quad \omega = \frac{\gamma}{v} \sqrt{v^2 t^2 - (x - x_i)^2}. \quad (23)$$

- It is easier to work in the Laplace domain. The **integral of the Green's function** over the half-infinite line have particularly simple forms

$$\tilde{U}(z, s) = \int_0^\infty \tilde{G}(x, -z, s) dx. \quad (24)$$

$$\tilde{U}(z, s) = \frac{\exp\left(-z \frac{\sqrt{s(s+2\gamma)}}{v}\right)}{2s},$$

$$\tilde{U}^\pm(z, s) = \frac{e^{-\frac{z\sqrt{s(s+2\gamma)}}{v}}}{2s} \left(1 \pm \frac{s}{\sqrt{s(s+2\gamma)}} \right). \quad (25)$$

Jose, Rosso and Ramola, *arXiv:2310.16811 (2023)*.

$t \rightarrow 0$	$t \rightarrow \infty$	
$\rho v f^+ t - \frac{\rho v \gamma}{4} (3f^+ - f^-) t^2$	$\rho \sqrt{\frac{D_{\text{eff}} t}{\pi}}$	annealed ρ , annealed m
$\rho v f^+ t - \frac{\rho v \gamma}{4} (3f^+ - f^-) t^2$	$\rho \sqrt{\frac{D_{\text{eff}} t}{\pi}}$	annealed ρ , quenched m
$\frac{\rho v \gamma}{4} (3f^+ + f^-) t^2$	$\rho \sqrt{\frac{D_{\text{eff}} t}{2\pi}}$	quenched ρ , quenched m
$\rho v f^+ (1 - f^+) t + \frac{\rho v \gamma}{4} (3f^+ - f^-) (f^+ - f^-) t^2$	$\rho \sqrt{\frac{D_{\text{eff}} t}{2\pi}}$	quenched ρ , annealed m

Table: Limiting behaviors of fluctuations for different initial conditions. Here, $D_{\text{eff}} = v^2/(2\gamma)$ is the effective diffusion constant for RTP motion in one dimension.

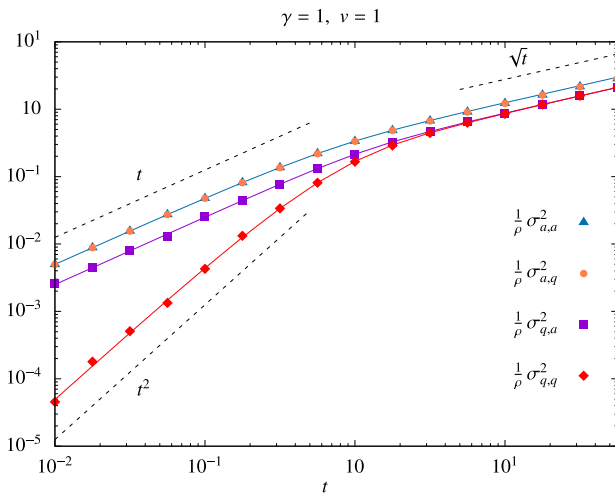


Figure: Variance of the integrated current plotted as a function of time for different initial conditions. The solid curves correspond to exact analytic results and the points are from numerical simulations of the microscopic model. For quenched density and quenched magnetization initial conditions, the fluctuations surprisingly exhibit a t^2 behavior at short times.

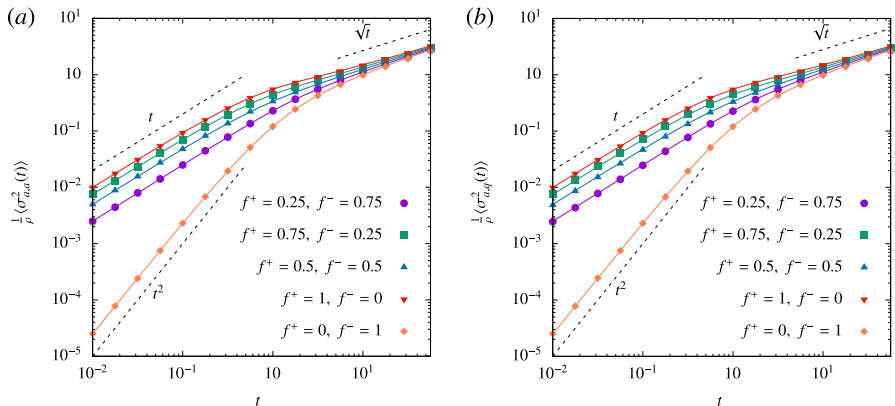


Figure: Variance of the time-integrated current plotted for annealed density initial conditions. The points are obtained from direct numerical simulations and the solid curves correspond to the exact analytical results. These plots are for the parameters $\rho = 20$, $\gamma = 1$, $\nu = 1$. The simulation data is averaged over 10^6 realizations.

1 Non-interacting active particle model

2 Effect of initial conditions

3 Interacting active lattice gas model

4 Conclusions

Dynamical rules	Rate
$\mu_i \leftrightarrow \mu_{i+1}$	D
$\mu_i \leftrightarrow \mu_{i+1}$, if $\mu_i^+ = 1$ and $\mu_{i+1} = 0$	λ/L
$\mu_i \leftrightarrow \mu_{i-1}$, if $\mu_i^- = 1$ and $\mu_{i-1} = 0$	λ/L
$\mu_i \rightarrow -\mu_i$, if $\mu_i \neq 0$	γ/L^2

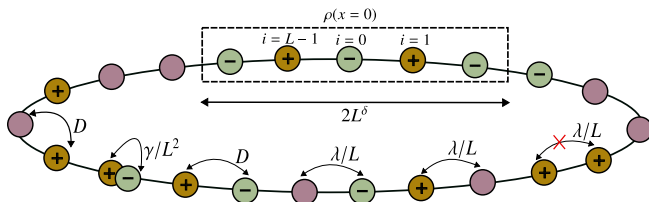


Figure: Lattice model of interacting active particles with different probability rates.

Kourbane-Houssene, Erignoux, Bodineau, and Tailleur, Phys. Rev. Lett. 120, 268003, (2018).

- Using the **diffusive rescaling** of space and time $x \rightarrow i/L$ and $t \rightarrow t/L^2$, one can define the coarse-grained plus and minus density fields $\rho^+(x, t)$ and $\rho^-(x, t)$ as

$$\begin{aligned}\rho^+(x, t) &= \frac{1}{2L^\delta} \sum_{|i-Lx| < L^\delta} \mu_i^+, \\ \rho^-(x, t) &= \frac{1}{2L^\delta} \sum_{|i-Lx| < L^\delta} \mu_i^-. \end{aligned} \quad (26)$$

- The **hydrodynamic equations** obeyed by the system are

$$\begin{aligned}\partial_t \rho^+ &= D \partial_x^2 \rho^+ - \lambda \partial_x [\rho^+ (1 - \rho)] + \gamma (\rho^- - \rho^+), \\ \partial_t \rho^- &= D \partial_x^2 \rho^- + \lambda \partial_x [\rho^- (1 - \rho)] + \gamma (\rho^+ - \rho^-). \end{aligned} \quad (27)$$

Agranov, Ro, Kafri, and Lecomte, J. Stat. Mech. 2021(8):083208, (2021).

- The **fluctuating hydrodynamic equations** obeyed by $\rho^+(x, t)$ and $\rho^-(x, t)$ can be written as

$$\begin{aligned}\partial_t \rho^+ &= D \partial_x^2 \rho^+ - \lambda \partial_x [\rho^+(1 - \rho)] + \gamma(\rho^- - \rho^+) + \frac{\sqrt{D}}{\sqrt{L}} \partial_x \eta^+ + \frac{\sqrt{\gamma}}{\sqrt{L}} \eta_K, \\ \partial_t \rho^- &= D \partial_x^2 \rho^- + \lambda \partial_x [\rho^-(1 - \rho)] + \gamma(\rho^+ - \rho^-) + \frac{\sqrt{D}}{\sqrt{L}} \partial_x \eta^- - \frac{\sqrt{\gamma}}{\sqrt{L}} \eta_K.\end{aligned}\quad (28)$$

- Mapping to **ABC model**

$$\begin{aligned}\langle \eta^\pm(x, t) \eta^\pm(x', t') \rangle &= 2\rho^\pm(1 - \rho^\pm) \delta(x - x') \delta(t - t'), \\ \langle \eta^+(x, t) \eta^-(x', t') \rangle &= \langle \eta^-(x, t) \eta^+(x', t') \rangle = -2\rho^+ \rho^- \delta(x - x') \delta(t - t').\end{aligned}\quad (29)$$

Scaled hydrodynamic equations

- In terms of the total density $\rho = \rho^+ + \rho^-$ and magnetization $m = \rho^+ - \rho^-$ fields, the hydrodynamic equations can be rewritten as

$$\begin{aligned}\partial_t \rho &= D \partial_x^2 \rho - \lambda \partial_x [m(1 - \rho)], \\ \partial_t m &= D \partial_x^2 m - \lambda \partial_x [\rho(1 - \rho)] - 2\gamma m.\end{aligned}\tag{30}$$

- Using a second rescaling $t \rightarrow t\gamma$ and $x \rightarrow x\ell_s$ where $\ell_s = \sqrt{\gamma/D}$, the above equations can be converted to the dimensionless form

$$\begin{aligned}\partial_t \rho &= \partial_x^2 \rho - \text{Pe} \partial_x [m(1 - \rho)], \\ \partial_t m &= \partial_x^2 m - \text{Pe} \partial_x [\rho(1 - \rho)] - 2m.\end{aligned}\tag{31}$$

- Activity is controlled by **Péclet number**, $\text{Pe} = \lambda/\sqrt{\gamma D}$
- The fluctuating hydrodynamic equations become

$$\begin{aligned}\partial_t \rho &= D \partial_x^2 \rho - \lambda \partial_x [m(1 - \rho)] + \frac{\sqrt{D}}{\sqrt{L}} \partial_x \eta_\rho, \\ \partial_t m &= D \partial_x^2 m - \lambda \partial_x [\rho(1 - \rho)] - 2\gamma m + \frac{1}{\sqrt{L}} \left(\sqrt{D} \partial_x \eta_m + 2\sqrt{\gamma} \eta_\kappa \right).\end{aligned}\tag{32}$$

Phase diagram

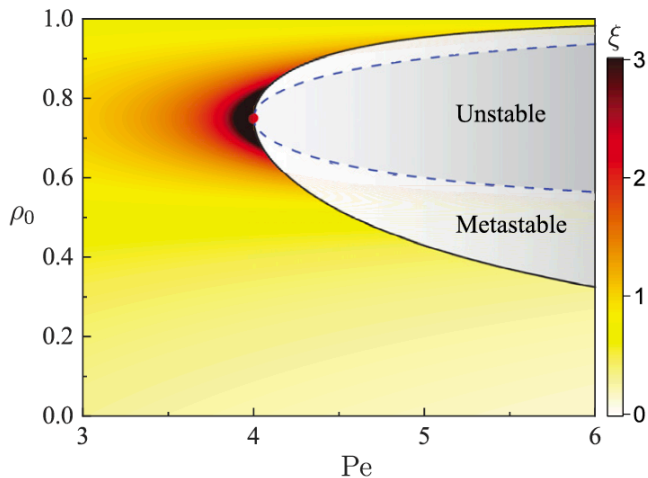


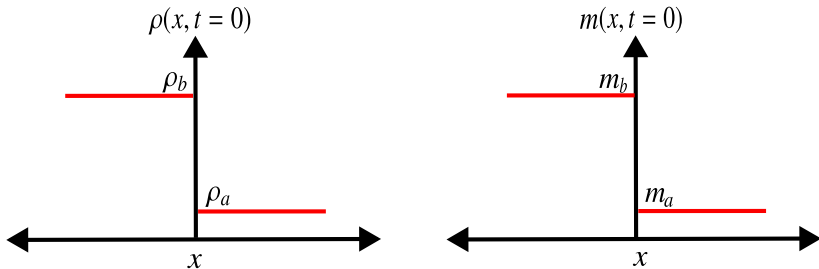
Figure: Linearly stable region is given by $Pe^2(1 - \bar{\rho})(2\bar{\rho} - 1) < 2$.

Agranov, Ro, Kafri, and Lecomte, J. Stat. Mech. 2021(8):083208, (2021).

Quenched initial conditions

- We consider quenched initial conditions of the form

$$\begin{aligned}\rho(x, 0) &= \rho_b \theta(\ell_s/2 - x) + \rho_a \theta(x - \ell_s/2), \\ m(x, 0) &= m_b \theta(\ell_s/2 - x) + m_a \theta(x - \ell_s/2).\end{aligned}\tag{33}$$



$$Q(t) = \int_{\frac{\ell_s}{2}}^{\ell_s} dx [\rho(x, t) - \rho(x, 0)].\tag{34}$$

Flat Initial Conditions: small and large time asymptotics

- In the limit of small T , we obtain

$$\langle Q(T)^2 \rangle_c \xrightarrow{T \rightarrow 0} \sqrt{T} \frac{\sigma_{\bar{\rho}}}{\sqrt{2\pi}}, \quad (35)$$

- where

$$\sigma_{\rho} = 2\rho(1 - \rho) \quad (36)$$

- and in the limit of large T , we obtain

$$\langle Q(T)^2 \rangle_c \xrightarrow{T \rightarrow \infty} \sqrt{T} \frac{\sigma_{\bar{\rho}}}{\sqrt{2\pi}} \frac{\xi(2 + \text{Pe}^2(1 - \bar{\rho}))}{\sqrt{2}}, \quad g \leq 2, \quad (37)$$

where

$$\xi = \frac{1}{\sqrt{2-g}}, \quad g = \text{Pe}^2(1 - \bar{\rho})(2\bar{\rho} - 1). \quad (38)$$

Jose, Dandekar, and Ramola, J. Stat. Mech. 083208 (2023)

- We obtain the following limiting behaviors

$$\langle Q(T)^2 \rangle_c \xrightarrow{T \rightarrow \infty} \sqrt{T} \frac{2\sqrt{|g_0|} \lambda (1 - \bar{\rho}) \bar{\rho}}{\sqrt{\pi} \sqrt{\gamma} (1 - 2\bar{\rho})}, \quad g_0 \leq 0,$$

and

$$\langle Q(T)^2 \rangle_c \xrightarrow{T \rightarrow 0} T^2 \frac{2\sqrt{|g_0|} \gamma \lambda (1 - \bar{\rho}) \bar{\rho}}{(1 - 2\bar{\rho})}, \quad g_0 \leq 0.$$

$$g_0 = (1 - \bar{\rho})(2\bar{\rho} - 1).$$

- To obtain the non-interacting limit, we take a $\bar{\rho} \rightarrow 0$ limit

$$\langle Q(T)^2 \rangle_c \xrightarrow{T \rightarrow \infty} \sqrt{T} \frac{\sqrt{D_{\text{eff}}}}{\sqrt{2\pi}} 2\bar{\rho}, \quad (39)$$

$$\langle Q(T)^2 \rangle_c \xrightarrow{T \rightarrow 0} T^2 2\gamma \lambda \bar{\rho}, \quad (40)$$

where $D_{\text{eff}} = 2\lambda^2/\gamma$ is the effective diffusion constant for a single RTP in 1D.

Match with hydrodynamic equations

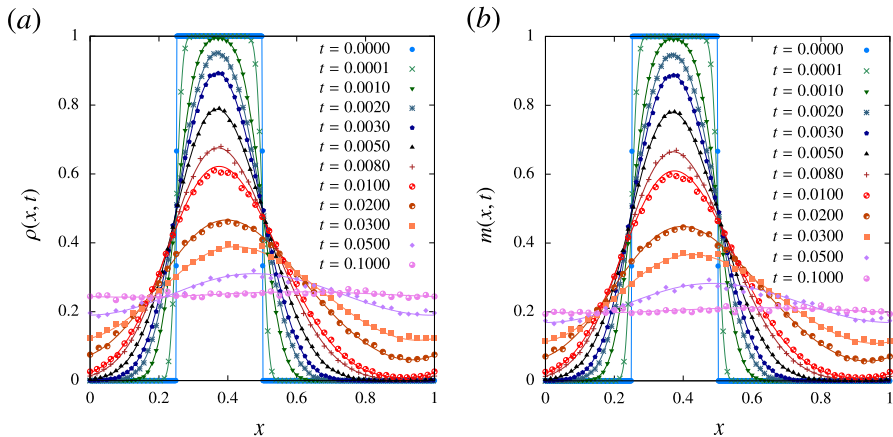


Figure: Evolution of the density $\rho(x, t)$ and magnetization $m(x, t)$ fields starting from a step initial condition for fixed parameter values $D = 1$, $\lambda = 5$, $\gamma = 1$. In the microscopic simulations, we have used a lattice of size $L = 1000$ with 250 particles.

Match with short time asymptotics and lattice effects

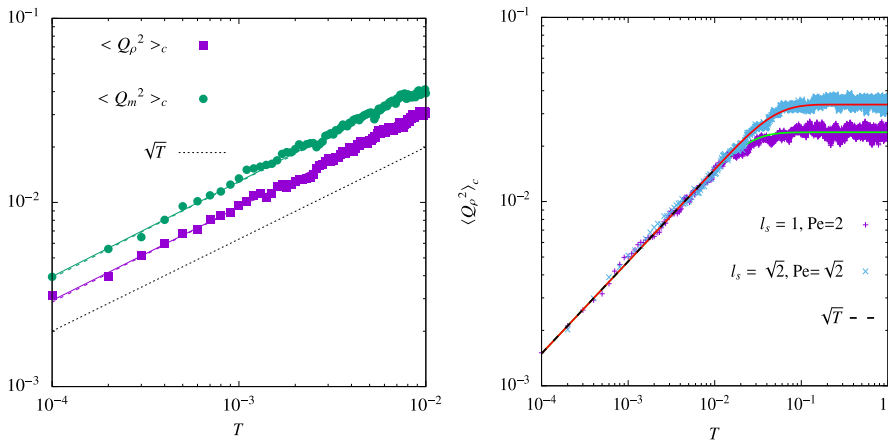


Figure: Second cumulant of the integrated current plotted as a function of time for the flat initial profiles with $\rho(x, 0) = 0.25$. The parameter values used are $D = 1$, $\gamma = 1$ and $\lambda = 10$. The points are obtained from MC simulations.

Three regimes and effect of density

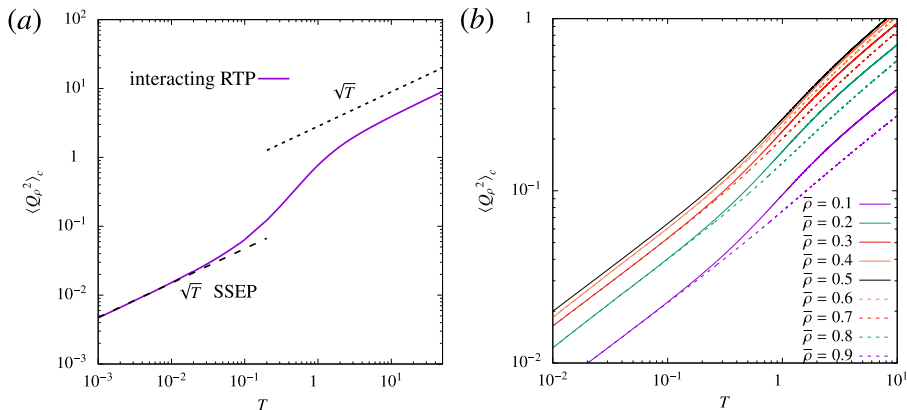


Figure: (a) Three regimes in the second cumulant for the initial condition $\rho(x, 0) = \bar{\rho} = 0.25$ and $m(x, 0) = 0$. (b) Second cumulant of the integrated density current plotted for the initial condition $\rho(x, 0) = \bar{\rho}$ and $m(x, 0) = 0$ for different values of $\bar{\rho}$. The Pe number is fixed to be 2.

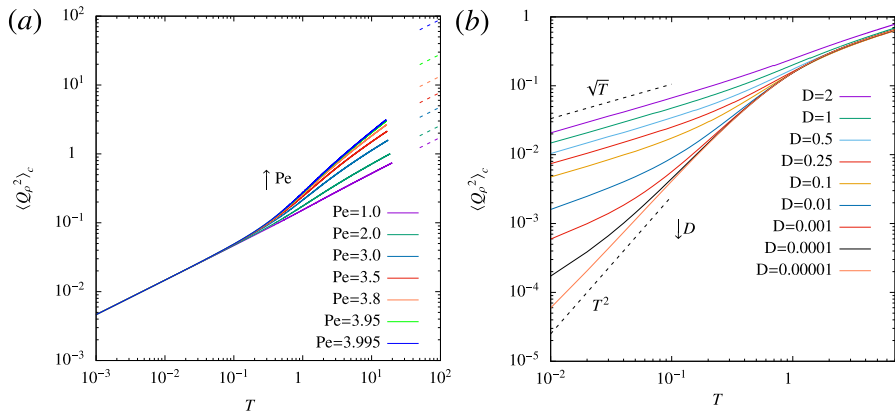


Figure: (a) Second cumulant of the integrated density current plotted for the initial condition $\rho(x, 0) = 0.75$, $m(x, 0) = 0$ for different values of Pe. (b) Second cumulant of the integrated density current plotted for the initial condition $\rho(x, 0) = 0.25$, $m(x, 0) = 0$ for different values of D. The fixed parameter values used are $\gamma = 1$, $\lambda = 2$. As we reduce D, the small time behavior changes from \sqrt{T} to T^2 .

- We analytically computed the current fluctuations across the origin for non-interacting RTPs. We also analytically computed the current fluctuations for an **interacting active lattice gas**.
- We showed that an **asymmetry in the initial bias directions** can lead to a **different power-laws** for the current fluctuations.
- The cumulants of the time-integrated current for the interacting active lattice gas model match the non-interacting case **at low densities**.
- It would be interesting to study generalized disorder averages in other models where multiple coupled fields appear.

Thank You.